REVIEW ARTICLE

A REVIEW ON CATALYST FORMULATION, REACTION CONDITION AND REACTION MECHANISM FOR DRY REFORMING OF METHANE/BIOGAS TO SYNGAS

Abdul Hadi Abdullah[a,b], * Ahmad Zamani Ab Halim[a], Amri Hj. Mohamed[b]

[a] Faculty of Industrial Sciences & Technology, College of Computing and Applied Science, Universiti Malaysia Pahang, 26300 Gambang. Kuantan. Pahang. Malaysia
[b] Faculty of Engineering, University College TATI, 24000 Kemaman, Terengganu.
Corresponding Author E-mail: abdulhadi@uctati.edu.my; aabdullah8761@gmail.com

ARTICLE DETAILS

ABSTRACT

Syngas production using methane dry reforming is a promising method that needs more exploration due to the benefits of harnessing the two most dangerous greenhouse gases, carbon dioxide and methane. The process can also employ biogas as a feed gas, which has a methane-to-carbon dioxide ratio of 1.5. However, due to the highly endothermic nature of the dry reforming reaction, a large quantity of energy is required. It has been demonstrated that the catalyst can be applied to lower the energy barrier and hence lower the reaction temperature. Many researchers have studied catalysts for dry reforming of methane. Coke deposition and active metals sintering are two conditions that can affect catalyst effectiveness. Many studies have claimed that the manipulated variables must be regulated in order to obtain an optimum catalyst for methane dry reforming. The impact of variables on catalyst performance was highlighted and thoroughly examined in this paper. The variables were separated into two groups: catalyst formulation variables and dry reforming reaction operating variables. Furthermore, this paper examined the potential of response surface methodology as techniques for determining the optimal variables with the fewest number of experiments and least expensive. This study also explored the reaction mechanism of dry reforming of methane over catalyst in order to get a better understanding of the essential path that the reaction takes.

KEYWORDS

Biogas Upgrading, Catalyst, Dry Reforming.

1. INTRODUCTION

Biogas is a renewable energy source that is produced by the anaerobic breakdown of biomass. It is mostly made up of methane (CH_4) (35-75%) and carbon dioxide (CO_2) (25-55%), with minor amounts of nitrogen (N_2), ammonia (NH_3), hydrogen (H_2), and hydrogen sulphide (H_2S) (Gao et al., 2020). Biogas is an important component of the emerging renewable energy market, and biogas utilisation is gaining traction in the renewable energy industry. Knowing that biogas is mostly made of CH_4 and CO_2, dry reformation of methane (DRM) for the production of synthesis gas (syngas) is a highly viable technology for its utilisation (Kalai et al., 2018). Currently, biogas is mainly used for heat and electricity generation, which has a low commercial value; however, this can be changed by adopting a dry reforming method to increase the market value of biogas (Jung et al., 2020). The CO_2 reforming of methane creates syngas with an equimolar CO/H_2 mix. For countries with limited sequestration options, using CO_2 and biogas to produce fuels and chemicals is an appealing option. As a result, innovations that can reduce CO_2 and CH_4 emissions are extremely important to the scientific community, policymakers, and governments (Ponugoti and Janardhanan, 2020). Overall, using biogas as a feedstock for the dry reforming of methane has environmental, health, and social economic benefits.

2. DRY REFORMING OF METHANE

The benefits and drawbacks of currently used methods for producing syngas were reviewed by (Abdullah et al., 2017). Because it uses two major greenhouse gases (CO_2 and CH_4), DRM has more potential than steam reforming (SR), partial oxidation (POX), and autothermal reforming (ATR) technologies to generate syngas. Syngas is vital to industry and can reduce greenhouse gas emissions overall (Afzal et al., 2018). In addition, some researchers proposed that DRM provides an appealing pathway to the economically beneficial sequestration of CO_2 via conversion to value-added chemicals and fuels (Afzal et al., 2018). The absence of an additional stream of oxygen or hydrogen gas means that DRM does not necessitate the removal of these components from the final product.

Previous research indicates that DRM can produce high-quality syngas with an H_2/CO ratio near to unity (Das, 2018; Pham et al., 2022; de Araujo Moreira et al., 2021; Moogi et al., 2022; Chamoumi et al., 2017). Furthermore, the input gas and reaction temperature can be adjusted to provide a range of product yield quality. The major result of the DRM reaction is syngas, which may be fed into the Fisher-Tropsch process to produce a variety of valuable products such as olefins and aromatics (Zhai, 2021). DRM can also use biogas as a feedstock. A group researchers stated in a review study that using biogas as a feedstock for the synthesis of renewable chemicals can be a more valuable method (Jung et al., 2020).

Biogas dry reforming reaction (Equation 1) is a strongly endothermic reaction, it needs a lot of heat to keep highly reactive A catalyst is a substance that is used to reduce activation energy and accelerate chemical reactions. However, side reactions on the catalyst's surface such as water gas shift (Equation 2), CO methanation (Equation 3), Boudouard (Equation 4), carbon gasification (Equation 5), carbon oxidation (Equations 6 and 7)

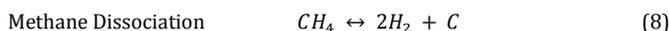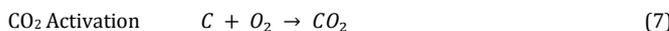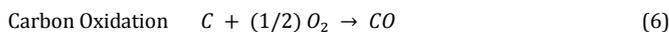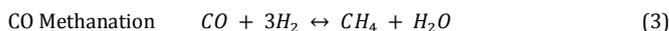and methane dissociation (Equation 8) can affect catalyst activity, selectivity, and stability. (Charisiou et al., 2018). The reactions that lead to the formation of carbon (Equation 4, Equation 5 and Equation 8) are favoured at low temperatures.

Methane Reforming	$CH_4 + CO_2 \leftrightarrow 2CO + 2H_2$	(1)
Water Gas Shift	$CO + H_2O \leftrightarrow CO_2 + H_2$	(2)
CO Methanation	$CO + 3H_2 \leftrightarrow CH_4 + H_2O$	(3)
Boudouard	$2CO \leftrightarrow CO_2 + C$	(4)
Carbon Gasification	$C + H_2O \leftrightarrow CO + H_2$	(5)
Carbon Oxidation	$C + (1/2) O_2 \rightarrow CO$	(6)
CO₂ Activation	$C + O_2 \rightarrow CO_2$	(7)
Methane Dissociation	$CH_4 \leftrightarrow 2H_2 + C$	(8)
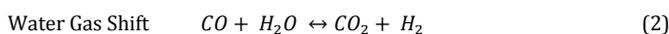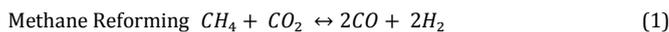
3. INFLUENCE OF VARIABLES ON CATALYST FORMULATION

A material that affects the rate of a chemical reaction in either a positive or negative way without being altered by the process itself is called a catalyst (Das, 2018). A catalyst, which speeds up the process, can reduce the activation energy required for a reaction. But the catalyst has no effect on how the products and reactants are distributed out during the equilibrium state. The physical and chemical properties of catalytic materials, according to a group researcher are critical for catalytic reactions because they can directly influence the surface adsorption and desorption of reactive species (Pham et al., 2022). Chemical properties include acidity and oxidation state of the active catalytic phase, whereas physical features include surface area, pore structure, density, and mechanical properties.

An active phase, a promoter, and a support are the three main components of a heterogeneous catalyst (de Araujo Moreira et al., 2021). Activating phases in reforming processes are often transition metals like nickel and platinum. Trace quantities of promoters are introduced to boost or keep constant the catalytic surface area, hence increasing or maintaining reaction activity or stability. Supports are employed to distribute active sites over the surface and to maintain these phases thermally stable for long periods of time (Moogi et al., 2022). Several noble and transition metals-based catalysts have recently been discovered to improve the endothermic reaction of methane dry reforming by improve catalytic activity and coke resistance (Abdullah et al., 2017). Noble metal catalysts such as Rh, Ru, Pt, and Pd metals are often utilised and more resistant to carbon formation than transition metals catalysts (Moogi et al., 2022). However, noble metal catalysts are often more expensive than transition metal catalysts as Ni, Co, Fe, and Cu metals (Chamoumi et al., 2017).

3.1 Noble Metal Catalyst

The main advantage of utilising a noble metal catalyst is that it reduces and modifies coke. The ability of noble metal catalysts to distribute on the support while yet maintaining a small particle size contributes to the optimum functioning (Khatri, 2021). A group researchers employed perovskite-supported Ru, Pt, and Pd catalysts for dry reforming of methane at ambient pressure and different reaction temperatures (400 to 800 °C) (Akansu et al., 2021). The catalytic capabilities of the catalyst were examined at various temperatures, and long-term studies were carried out to assess the catalysts' resistance to carbon deposition. The reaction took place at a a space velocity of 48 000 h⁻¹ by control total flow rate at 100 mlmin⁻¹ and 100 mg catalyst loading. Stable conversion of both CH₄ and CO₂ was observed after 50 hours of stability study over a Ru substituted LaAlO₃ catalyst. This suggests that it is a highly stable and coke-resistant DRM catalyst. The deactivation of Pt and Pd combined with LaAlO₃ as a result of sintering and carbon deposition is demonstrated by TEM and STEM data. The highly stable Ru catalyst was primarily due to the strong contact between Ru and Al, as proven by H₂-TPR and XPS findings. The product yield increases as the reaction temperature rises.

In addition, the surface properties of a catalyst are improved by the use of noble metals. The catalytic activity, stability, and surface characteristics of Pd-CeO₂ nanocrystals catalysts for the dry reforming of methane process were studied (Han et al., 2021). Simple surfactant induced technique was used to prepare Pd-CeO₂ nanocrystals. Researchers observed that the catalyst had excellent coke resistance and prevented deactivation from coke production during catalysis based on the results of an activity performance test. The catalyst performance at low temperature is the main advantage of Pd-CeO2 catalyst. Due to the presence of widely scattered and extremely small Pd-nanoparticles (2.9 nm), the catalyst demonstrated syngas production at around 350 °C. Images obtained using HRTEM (Figure 1) reveal that Pd-species with a deposit size of 1-15 nm

have been deposited on the surface of the support. Pd-dispersion study revealed that Pd-nanoparticles are considerably smaller in size. This finding demonstrates that a catalyst with a high dispersion of noble metals can improve its activity and stability.
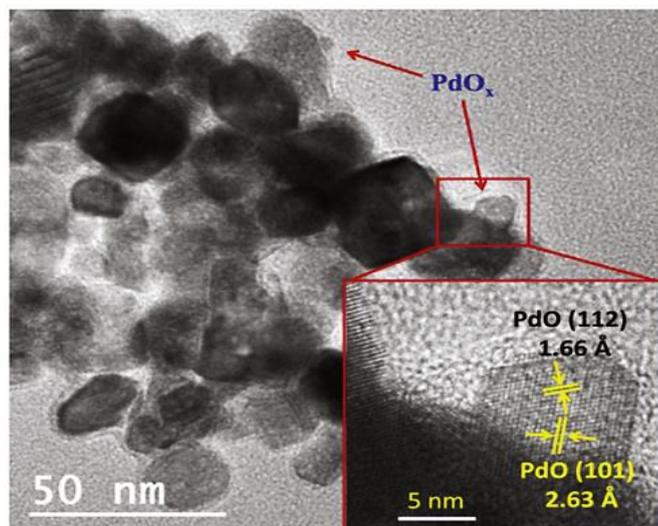

Figure 1: TEM images of Pd-CeO₂ nanocrystals catalysts (Singha et al., 2017).

In addition, noble metal catalysts can offer higher catalytic activity and stability by modifying the type of coke produced during the DRM reaction. Type of coke formed on the catalyst surface can change the particle size of active metals (Khatri, 2021). According to a recent article, significant interactions between the support and Rh inhibit metal sintering (Kumar et al., 2019). Furthermore, noble metals can limit the development of graphitic and destructive forms of carbon, demonstrating the ability of noble metal catalysts to modify the formation of coke (Ma, 2020). The strong coke resistance and catalytic activity of noble catalysts have been validated by several research, as shown in Table 1.

Despite noble metal-based catalysts' excellent resistance to coke deposition, as well as their remarkable stability and high catalytic activity, as described above, their practical usage has been severely hampered by their high cost due to the material's limited availability.

3.2 Non-Noble Metal Catalyst

Non noble metal catalysts (transition metals) were often used in the dry reforming of methane because of acceptable catalytic activity and less expensive compared to noble metals. When these catalysts are used, they produce a lot of coke, which makes them less effective and is a major operational disadvantage, even though they seem useful for industrial applications. But adding a few changes to a catalyst made of non-noble or transition metals can make it more stable and increase its catalytic activity.

A studied the catalytic performance of a monometallic Fe and Ni catalyst supported with MgₓAlᵧOᵤ matrix (Fogler, 2017). The support was prepared from a hydrotalcite-like precursor. The catalytic experiment of prepared catalyst was evaluated at 600 °C and ambient pressure in a packed-bed reactor The researchers discovered that graphitic carbon synthesis caused considerable deactivation of monometallic Ni catalysts. However, when compared to Ni catalyst, the DRM catalytic activity of Fe catalyst was relatively low.

In a separate work, employed MgO-supported monometallic Ni and Co produced by the incipient wetness impregnation technique for DRM reaction (Xie, 2020). The DRM reaction was carried out in a 14 mm-i.d. stainless-steel reactor at 800 °C. The researcher discovered that the Co/MgO catalyst had a smaller surface area and larger metal particles than the Ni/MgO catalyst. Furthermore, the TPR analysis revealed that Ni had a stronger interaction with support than Co.

Previous work on DRM via monometallic non-noble metals is summarised in Table 1. The non-noble metals catalyst fast deactivation can be avoided by increase the metal dispersion on the support or reduced the active metal particles size. The fundamental issue in commercialising DRM reactions in industry is the development of low-cost, high-activity catalysts that are resistant to carbon deposition (Abdullah et al., 2017). According to a survey of the relevant literature, the Ni catalyst has been widely employed for DRM reactions due to its excellent catalytic performance and low cost. However, at higher temperatures, Ni monometallic catalyst typically deactivates and sinters. Various solutions

to the problems have been investigated. Combining the two or more metals with different characteristic is the common method to increase the catalyst activity and stability.

3.3 Bimetallic Catalyst

Bimetallic or alloy catalysts may be able to address the issue of non-noble catalysts becoming inactive due to excessive coke formation while also cutting overall costs. Furthermore, it can improve a metal's dispersion and reduce particle size while keeping its catalytic activity and stability. According to a study, bimetallic can improve catalytic activities by increasing the dispersion and decreasing the size of the active metal particles (Abdulrasheed, 2019). Moreover, the catalyst prepared from bimetallic can improve the catalyst reducibility, prevent surface carbon formation, control the type of surface carbon and strengthen the interaction between the metals.

For DRM reactions, some researchers found that supported bimetallic catalysts exhibit high activity and stability (Taherian et al., 2021). After 50-150 hours on stream, a bimetallic Ni-Co catalyst supported on Hydroxyapatite produced using standard impregnation processes showed little deactivation. The researchers also noted that feed conversion increased with warmth. The feed CH_4 and CO_2 conversion increased by up to 10% as temperature increased by 50 °C in the tested temperature range of 700 °C to 750 °C and approximately 1.6 bar fixed bed reactor. On top of that, water's presence along the catalytic process is due to the water-gas shift reaction. The physical characterisation of used catalyst revealed low carbon production and no substantial change in particle size.

Carbon-resistance features of bimetallic catalysts can help increase the catalyst's stability. In a recent work, employed a bimetallic Ni-Ru active site for CO_2 reforming of methane (Aramouni et al., 2018). By combining Ni-Ru metals, the catalyst stability was significantly improved but the catalyst performance was slightly reduced. The experiment data show that the reduction of monometallic nickel catalyst was due to addition of ruthenium. This can happen when Ru atoms are on the step-edge sites of Ni particles and when these reactive step-edge sites on Ni surfaces are blocked. Typically, the active sites on nickel surfaces consist of terraces and edge-step sites. The reactivity of catalytic surfaces is usually dominated by step-edge sites, which are composed of highly reactive, low-coordinated atoms. Because of this, the presence of Ru reduces the catalytic activity. However, studies also revealed that the inclusion of Ru lowers CO_2 conversion, promotes the gasification of carbon-adsorbed species, and prevents the dissociation of CO, hence enhancing the catalyst's coke resistance.

Table 1 summarises additional benefits and significant effects of utilising bimetallic active site catalysts from previous work. Because of its superior catalytic capabilities, the Ni/Co combination is currently the most preferred approach. A studied the effect of Ni/Co ratio in DRM catalyst and found that it has a substantial effect on feed conversion and product quality due to H2 spill over (Anil et al., 2020). Furthermore, due to Co's high oxygen affinity, it contributed to the elimination of coke and whisker formation. The Ni/Co without support, on the other hand, has large particles that cause agglomeration.

Besides the active site, the DRM catalyst's catalytic activity and stability depended on the support. Support is important to improve the metal-support interaction, reduce the active metals particle size, prevent metals particle agglomeration, increase metals reducibility, and prevent coke formation. However, the physicochemical properties of support must be considered during support selection (Khatri, 2021).

3.4 Support

Catalysts require support materials with specific textural and physicochemical properties to stay uniformly distributed and carbon resistant. Supports with a large porous volume and surface area can improve the active metal dispersion (thus reduce particle size) are preferable for achieving high activity. Strong interaction between active metals and support can influence the stability and reducibility of catalyst. In most instances, a catalyst will consist of numerous components that must be combined in a particular way to get the desired structure. When making a supported metal catalyst, it is common practise to enclose the active metal within the support material. These supporting components are required for the catalytic process to take place. Support materials maximise the surface area of active sites by providing a large area over which metallic compounds can disperse; this, in turn, enables the catalyst's fine shape to be tailored to the reactor's particular needs (Abdullah et al., 2017).

Support inhibits metal aggregation by increasing the active metal-support interaction. A group researchers examined the performance of Ni nanoparticles of different sized supported on metal oxides (2.6, 5.2, 9.0, and 17.3 nm) (SiO_2, Al_2O_3, MgO, ZrO_2, TiO_2) (Singha et al., 2017). Due to the strong effect of particle size and support type on the catalytic activity and stability, the conversion rates of inlet feed under same reaction conditions vary significantly depending on the support employed. In addition, Ni nanoparticles were seen to be reduced at higher temperatures than SiO_2 overlayer, indicating that the connection between Ni and metal oxide overlayer was stronger. Nevertheless, not all metal oxides exhibit the same stability as catalysts at 800 °C. The Al_2O_3, ZrO_2, and MgO overlays displayed just a minor alteration, whereas the TiO_2 surface exhibited significant crystallisation and discrete oxide domains. The results of STEM indicate that Ni does not aggregate on Al_2O_3, ZrO_2, or MgO overlayers. However, the Ni that was coated with the TiO_2 overlayer exhibited significant nanoparticle aggregation.

Support also increases metal dispersion and reduces the crystallite size. In a study on the effect of support, Wysocka et al. found that, high BET surface area of SiO supported Ni catalyst was donated by high dispersion of active metal (Wysocka et al., 2019). In the same article, Al_2O_3 support did not affect the surface area and ZrO_2 caused the reduction of BET surface area from 30 m^2g^{-1} to 23 m^2g^{-1}. In addition, the size of NiO crystallite also varies according to the type of support. The XRD data showed that Ni/SiO has smaller crystallite size followed by Ni/Al_2O_3 (21 nm) and Ni/ZrO_2 (22 nm). However, the catalytic testing data indicated that there is no correlation between BET surface area and catalyst activity. The highest activity was observed for supports that strongly interact with active metals. By comparison, Al_2O_3 has strong interaction with Ni compared to ZrO_2 and SiO_2 support. More advantages and significant effect of using support can be found from published works (Figueire et al., 2018; Mofrad et al., 2019; de Vasconcelos et al., 2020; Erdogan et al., 2018). The dispersion and chemical states of Pd were the key determinants in the catalyst's high performance. From the characterization study, they concluded the high dispersion of Pd nanoparticles over the zeolite support.

In DRM reaction, there are several research which have been published on using zeolite as catalyst support (Chen et al., 2021; Kweon et al., 2022a; Liang et al., 2023; Najfach et al., 2021). Kweon et al. highlighted that, using zeolite support can increase Ni catalytic activity and stability (Kweon et al., 2022b). They compared the performance of Ni supported with zeolite and Al2O3 and reported that catalyst supported with zeolite exhibited higher conversions of both CH4 and CO2 and stability than the Ni/Al2O3 catalysts. The in-situ reduction impact on the zeolite framework is mainly responsible for the excellent performance of the Zi/Zeolite catalyst. In a review paper entitled Zeolite and clay-based catalysts for CO2 reforming of methane to syngas, Hambali et al. concluded that zeolite deserved the attention of using as catalyst support for DRM reaction (Hambali et al., 2022). They listed the advantages of zeolite such as availability, peculiar structures, high affinity for CO2, environmentally friendly nature, and tuneable properties to improve selectivity of target products thar should be utilized to produce ideal DRM catalyst.

Numerous crucial catalytic processes, including hydrogenation, Fisher-Tropsch synthesis, vehicle exhaust catalysis, and selective catalytic reduction, have been shown to be efficient employing zeolite-supported metal catalysts. Zeolites are microporous crystalline minerals composed of ordered formations of TO4 tetrahedra (T = Si/Al) with pores varying between 4 and 7.5. Their ordered microporous linked networks, hydrothermal stability, vast surface area, acidity, and cation exchange capacity are well-known. Zeolites are widely employed in gas separations (molecular sieving), ion exchange, adsorption, and catalysis (size and shape-selective catalysis) due to their unique structural features (Pan et al., 2020).

The zeolite support's ability to be tuned for acidity using metal clusters and nanoparticles is advantageous for enhancing the catalytic performance of diverse reaction processes. According to Limlamthong et al., metal encapsulation within the zeolite structure has been proposed as a feasible solution for catalytic instabilities that are resulted from metal coalescence, sintering and leaching (Limlamthong et al., 2020). There are several studies that have been done by using zeolite supported catalyst to enhance the reaction performance. Xie et al., investigated the performance of methane combustion over zeolite supported Pd catalysts with the lanthanum (Xie et al., 2021). Zeolite ZMS-5 was chosen for Pd catalyst support. They found that, the optimal catalyst stood out compared with other reported similar Pd catalysts for the catalytic combustion of methane in terms of activity. The dispersion and chemical states of Pd were the key determinants in the catalyst's high performance. From the characterization study, they concluded the high dispersion of Pd nanoparticles over the zeolite support.

In DRM reaction, there are several research which have been published on using zeolite as catalyst support (Chen et al., 2021; Kweon et al., 2022a;

Liang et al., 2023; Najfach et al., 2021). Kweon et al. highlighted that, using zeolite support can increase Ni catalytic activity and stability (Kweon et al., 2022b). They compared the performance of Ni supported with zeolite and Al_2O_3 and reported that catalyst supported with zeolite exhibited higher conversions of both CH_4 and CO_2 and stability than the Ni/Al_2O_3 catalysts. The in-situ reduction impact on the zeolite framework is mainly responsible for the excellent performance of the Zi/Zeolite catalyst. In a review paper entitled Zeolite and clay-based catalysts for CO_2 reforming of methane to syngas, Hambali et al. concluded that zeolite deserved the attention of using as catalyst support for DRM reaction (Hambali et al., 2022). They listed the advantages of zeolite such as availability, peculiar structures, high affinity for CO_2, environmentally friendly nature and tuneable properties to improve selectivity of target products thar should be utilized to produce ideal DRM catalyst.

Table 1: Recently developed noble catalysts for the DRM reaction.				
Catalyst	T (°C)	Conv. CH4 (%)	Remarks	References
Rh	550	45	Rh based catalyst has higher surface area compared to Ni based catalyst Rh reduction temperature is low compare to Ni Rh/Al catalyst exhibits slow deactivation and higher H2/CO rati.o	(Damyanova et al., 2020)
Ir	600-800	61	Carbon deposition and sintering of supports were linked to a decline in performance. Used catalysts did not exhibit iridium sintering. Ir/ Ce0.9La0.1O2(M = Pr, Zr) MDR catalysts were more stable than Ir/CeO2.	(Wang et al., 2017)
Ir	600	40	The shape of the supports made of $Ce_{0.9}La_{0.1}O_2$ changed the way the catalysts worked. In the Ir/ $Ce_{0.9}La_{0.1}O_2$-nanorods, the interaction between the metal and the support was improved. For the MDR reaction, the nanorod catalysts worked much better and were more stable.	(Wang et al., 2020)
Pt	200-400	100	Pt-free NiO exhibited the highest catalytic activity and showing 100% CH4 selectivity.	(Sápi et al., 2019)
Pd	650	65	Electroless Pd deposition was used to make a porous Pd-Ni-YSZ membrane. The Pd-Ni-YSZ (EPL) porous membrane was more stable and could handle carbon better. Pd clusters can stop carbon from building up on the surface of Ni.	(Lee et al., 2017)
Ru	750	94	Ru addition has positive effect on Ni/Al_2O_3 for DRM contrary to $Ni/MgAl_2O_4$ and Ni/YSZ. Addition of ruthenium on Ni/Al_2O_3 leads to an increase in the catalyst stability and efficiency by inhibiting the formation of poorly active phase $NiAl_2O_4$	(Andraos et al., 2019)
Ni	650	60	Ni/Mg(3)Al catalyst shows a reduction peak at 774ºC due to the reduction of NiO with an strong interaction with the support.	(Ocsachoque et al., 2017)
Fe	700	10	Fe10%Al2O3 are promising, cost-efficient, catalysts for biogas dry reforming. Fe segregation into strips owing to incomplete reduction induces reactivity loss.	(Jabbour et al., 2019)
Co	700	20	Sintering and Co oxidation reduce Co/SBA-15 activity. Samaria degrades catalyst in Co/SBA-15. At high temperatures, Samaria becomes SmCoO3 with acidic characteristics.	(Taherian et al., 2017)
Co	800	80	Co/CeO_2 shows the best selectivity at low temperature (600 °C) Studies show that replacing Ni with Co makes the metal less reactive towards methane	(Guerrero-Caballero et al., 2019)
Fe	800	20	Iron-doped DRM activity is minimal around 600–800 °C reaction temperature	(Guerrero-Caballero et al., 2019)
Mo	750	14	Alumina supported molybdenum catalysts show noticeable activity for dry reforming of methane. Increase Mo loading, increase the CH4 conversion at same reaction temp.	(Gaillard et al., 2017)
Zr	550	25	Zr species introduced in small amounts upon calcination stay in brucite-like layers. Ce/Zr molar ratio influenced catalysts properties (basicity, reducibility, texture etc.). Presence of Zr species in brucite-like layers inhibited C-forming reactions.	(Dębek et al., 2017)
Ni-Fe	848	50	Ni-Fe alloy nanoparticles had excellent carbon coking resistance Ni-Fe combination prevent metal sintering at 950 °C Ni-Fe effect on feed conversion is less significant but increase the catalyst stability	(Joo et al., 2020)
Ru-Ni	750	76	Ru increases the catalytic activity in 10% and leads to less coke deposition Bimetallic catalyst increases reducibility and dispersion of Ni, which indicate remarkable interaction between metals.	(Álvarez Moreno et al., 2021)
Ni-Co	750	70	Bimetallic Ni-Co catalyst were prepared from La(CoxNi1-x)0.5Fe0.5O3 precursors. The catalytic activity and coking resistance are both improved by a little amount of Co substitution. The amount of Co in the perovskite precursor determines its crystalline structure.	(H. Wang et al., 2019)
Pt-Ni	800	80	DRM reaction does not deactivate Pt-Ni/CeO2. Pt-Ni/CeO2 enhances CH4 conversion. Pt promotes metal dispersion and Pt-Ni/CeO2 reducibility. Pt-Ni/CeO2 resists coking.	(Araiza et al., 2021)
Mo-Ni	550-700	70	MoOx species to Ni increases electron density Mo-Ni bimetallic reduces whisker-type carbon deposited All Mo-doped catalysts form more CO	(Jawad et al., 2020)
Sn-Ni	700	40	Theoretical and experimental studies showcasing the stability of Ni-Sn bimetallic catalysts. The bimetallic catalysts are more stable over time and can handle more carbon than the monometallic ones.	(Guharoy et al., 2018)

3.5 Promoter

As discussed in the previous section, one of the main issues in DRM catalyst development is the reduction of catalyst activity and stability due to coke formation. The addition of promoters such as alkaline earth metal oxides is a promising method for the reduction of coke formation during DRM reaction. Promoters are the small amount of active ingredients that are added to the catalyst for improving catalyst activity.

Recently, the base promoter has been used to enhance the DRM catalyst activity and stability because base promoter can enhance the CO_2 absorption and suppress the sintering of catalyst. Promoter increases the catalyst activity by improving the catalyst surface properties. Nisa et al. investigated the effect of base promoter (Mg, Ca, Na and K) on the Ni/MCM-41 catalyst (Nisa et al., 2022). They concluded that, Ni/MCM-41 promoted with Mg has the highest feed conversion due to basic properties of catalyst surface. The basicity of catalyst was measured by the amount of CO_2 adsorption during CO_2-TPD analysis. In addition, promoter also affected the reducibility of catalyst and base promoter replenishment increases the total H_2 consumption. From H_2-TPR analysis, catalyst that was promoted with Mg and Na shows the highest amount of H_2 consumption. In overall, the catalytic activity test showed the catalyst that was promoted with 5 %Mg has better catalyst activity and stability for DRM.

MgO promoter can improve the interaction between support and active site. Taherian et al. discovered that the interaction between Ni and SBA-16 support is enhanced by the addition of promoter on Ni/SBA-16-MgO catalyst (Moogi et al., 2022). Strong interaction between Ni and support was donated by the presence of reduction peak at 600 °C during H_2-TPR analysis. Strong Ni-support interaction is important to eliminate the aggregation of Ni particles. More advantages of using promoter in DRM catalyst can be referred to literature (Ocsachoque et al., 2017; Abdulrasheed et al., 2020; Ghani et al., 2018; Sun et al., 2019; Park et al., 2018).

3.6 Other Techniques

Besides active metals, support, and promoter; other techniques have been introduced to improve the catalytic activity of DRM catalyst. For example, the effect of support preparation routes and metals addition sequence have been used to increase the catalytic activity and stability (de Souza, 2022; Shin, 2018; Abdullah, 2020). Yusuf et al. , investigated the effect of Ni/Al$_2$O$_3$-MgO catalyst preparation route of DRM reaction (Yusuf et al., 2021). The catalysts were prepared by co-precipitation and co-precipitation which was followed by impregnation methods. They found several important effects of prepared catalysts on the catalyst properties and performance. Firstly, catalyst that is prepared by two-step method has higher initial feed conversion (X_{CH4}=60 %; X_{CO2}=70 %) compared to co-precipitation synthesis catalyst (X_{CH4}=50 %; X_{CO2}=60 %) at same reaction condition. Secondly, the initial H_2/CO ratio for catalyst prepared by co-precipitation was lower than unity. Third, carbon measurement on spent catalyst showed the higher amount of carbon deposited on Ni/Al$_2$O$_3$-MgO catalyst prepared by co-precipitation. In addition, the catalyst preparation route can influence the catalyst textural properties such as surface area and particles size.

Metal loading on catalyst is also a significant factor that needs to consider during catalyst preparation. Metal loading percentages can affect the metal dispersion, agglomeration, catalyst surface area, metal-support-promoter interaction strength and other properties. It is important to have an optimum loading percentage in order to maximize the feed conversion and increase catalyst stability. Investigation of metal loading is common in DRM catalyst research. Zhang et al. examined the Ni loading effect on DRM catalyst (Zhang et al., 2021). They used robust nanosheet-assembled Al$_2$O-supported Ni catalysts for the dry reforming of methane. The Ni content was varied between 3-20 % and they found that enhancing the loading of Ni increases the Ni nanoparticle size and initial catalytic activity, which simultaneously declines the nickel dispersion and the interaction between Ni and the support. Based on their experimental works, catalyst loading with 5 % Ni shows optimum result.

In another studies, the effect of secondary Co metal on TiO based catalyst was investigated by Mazhar et al. (Mazhar et al., 2021). They reported that the that was catalyst loaded with 5 % Co as secondary metals has the best activity performance. The 5%Co/TiO$_2$–MgAl$_2$O$_4$ improved the CH$_4$ and CO$_2$ conversion up to 70% and 80%, respectively, while the selectivity of H$_2$ and CO improved to 43% and 46.5%, respectively. The main reason the catalyst works so well is that Co interacts strongly with the support. In addition, the higher Co loading adhered to the issue of carbon deposition because the larger amount of available carbon species led to deactivation.

Based on literature review, the most study loading range for Ni is between 1 to 10 % (Sharifianjazi et al., 2021). The most study loading range for cobalt and promoter loading is between 0 to 10 % is between 0 to 10 % 0 to 5 % respectively (Al-Fatesh et al., 2022; Bagabas et al., 2021; Tran et al., 2021; Yentekakis et al., 2021).

4. INFLUENCE OF DRM OPERATING CONDITION

As discussed in previous section, a catalyst plays an important role in DRM. The high catalytic activity and stable catalyst will increase the efficiency of DRM process and the quality product syngas. Another factor that is important in DRM process is operating condition. The optimum operation condition will optimize the efficiency and cost of DRM process. Thus, it is important to review the interaction behaviour between the operation condition and the DRM efficiency (or catalyst efficiency). The influences of operating conditions such as reduction temperature, reaction temperature and gas hourly space velocity (GHSV) were discussed in the following sub-topics.

4.1 Influence of Reducing Environment on Catalytic Activity

Pre-treatment has a significant role in the formation of active metal sites, thus influencing the performance of catalysts. Some researchers indicated the formation of metallic nickel through the reduction of nickel oxide with CO as shown in the following equation (Cabascango and Bazhin, 2020):

$$NiO(solid) + CO(gas) \rightarrow Ni(solid) + CO_2(gas) \qquad (9)$$

Various reducing atmospheres (CO, CH$_4$, He and H$_2$, N$_2$, H$_2$-N$_2$, H$_2$-He) were investigated for their influence over catalytic activity. Al-Fatesh et al. (Al-Fatesh et al., 2019) investigated the effect of in-situ and ex-situ reduction on catalytic activity of Al$_2$O$_3$-ZrO$_2$ supported Ni-Co for dry reforming of methane under H$_2$ flow at 800 °C for 1.5 h. They reported that catalyst treated with ex-situ reduction has higher catalytic activity compared to in-situ reduction.

The development of active metal sites depends critically on pre-treatment prior to the reaction. This parameter modifies the shape and size of metal particles as well as the contact between the metal and the support, which in turn has an effect on the catalytic efficacy of catalysts. The catalytic performance of the dried catalyst was evaluated by Rego de Vasconcelos et al. who compared it to the performance of the in-situ reduced catalyst (de Vasconcelos et al., 2020). The in-situ reduction was performed at 700 °C for 1 h under 4 % H$_2$/N$_2$ flow. According to their result, the feed conversion of catalyst with in-situ reduction was slightly higher than only drying treatment. However, the catalyst that did not have in-situ reduction lost its activity a lot more quickly. The researchers had a theory that the improved catalytic performance achieved with the reduced catalyst at the beginning of the experiment may be attributable to the reduction of nickel particles to a larger degree prior to the DRM. Consequently, the active phase Ni^0 would be produced, which would then convert the reactants that were present at the beginning of the DRM process. It is possible that the environment that is present during DRM is insufficient to fully reduce nickel oxide particles, especially those with stronger metal-support interactions. This might be the reason why the catalyst deactivates so quickly.

Figure 2 shows the comparison of TEM image for catalyst that calcined before reduce and direct reduction (skip calcined steps) under H$_2$ atmosphere at 800 °C (Zhou et al., 2018). From the image it could be concluded that, the catalyst with direct reduction has smaller particles size compared to the catalyst that is calcined and reduced. The catalyst activity result showed that the catalyst with direct reduction has slightly higher initial CH$_4$ conversion but deactivated faster than the catalyst that is calcined and reduced.

The catalyst activity and characteristics can also be affected by the reduction temperature. The reduction temperature is often related to the amount of metal oxide reduced to metal crystallite. Zhou et al. studied the influence of reduction temperature on catalyst activity (Moreno et al., 2021). Figure 3 depicts the activity of the Ni/CeO$_2$ catalyst on DRM at different in-situ H$_2$ reduction temperatures, namely 400 °C, 600 °C, 700 °C, and 800 °C. Ni/CeO$_2$ treated in-situ at 400 and 600 °C showed comparable reactant conversion trends over 24 h. Reduction temperatures of 700 °C and 800 °C resulted in rapid catalytic activity decrease trends in the first 2 hours and a low conversion of reactants throughout the catalytic testing. Based on their findings, they concluded that high H$_2$ reduction temperatures resulted in complete reduction of NiO and CeO$_2$ phases in Ni/CeO$_2$ catalysts while Ni/CeO$_2$ catalysts that were reduced in-situ by H$_2$ at 400 °C resulted in partial reduction of NiO. In addition, a pre-treatment with hydrogen at a temperature of 600 °C may reduce the amount of surface CeO$_2$ and some of the NiO phase in the sample.

Moreover, the quick deactivation of the Ni/CeO₂ catalyst following in-situ H₂ reduction at 700 °C and 800 °C suggested that the Ni⁰ supported by CeO₂ₓ phase was not highly reactive on DRM streams. It is possible to conclude that the reduction temperature has an effect on both feed conversion and the H/CO ratio. Higher feed conversion and H₂/CO values were obtained at low temperatures (400-600 °C), while lower feed conversion and H₂/CO values were obtained at higher temperatures (700-800 °C). The influence of reduction temperature on feed conversion and H₂/CO was not significant when compared to the low temperature (400 °C and 600 °C) and high temperature (700 °C and 800 °C) regions.
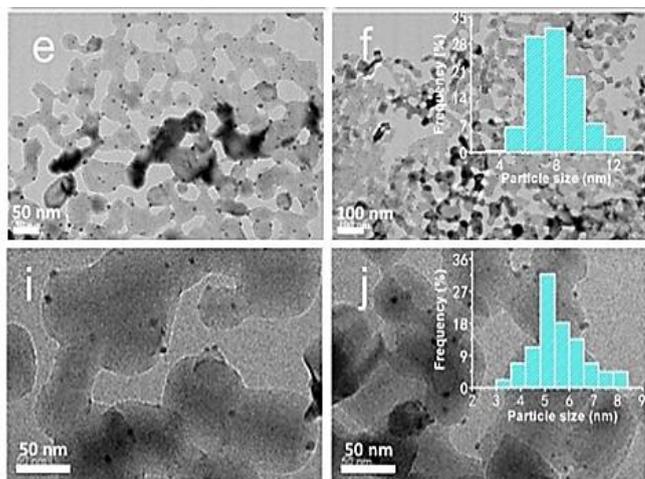
Figure 2: TEM micrographs and particle size distribution of reduced metallic particles for (a, b) calcined/reduced catalyst and (c, d) direct reduce catalyst (Zhou et al., 2018)
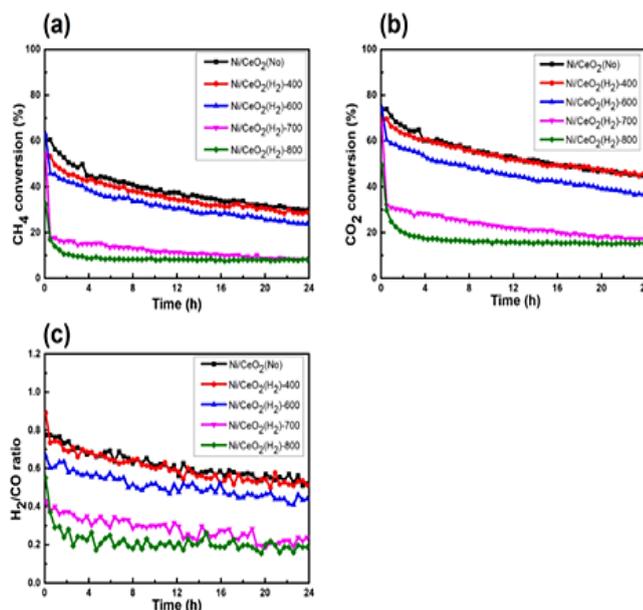
4.2 Influence of Reaction Temperature

Due to the endothermic nature of DRM, the reaction temperature has the most significant effect on catalyst activity. According to the hypothesis, the high temperature is in favour with the catalyst activity and increase the inlet feed conversion. Evaluation of different catalyst on DRM feed conversion at different temperature were carried out by Turap et al. (Turap et al., 2020). They reported that, all catalysts showed the highest catalytic activity at 850 °C and the feed conversion conversions increased with reaction temperatures. The same trend was observed on product H₂/CO ratio whereby, higher reaction temperature increases the H₂/CO ratio. Similar finding was reported by Lin et al. in which, the feed conversion of DRM reaction increased with temperature when the reaction temperature increased from 550 °C to 800 °C (Lin et al., 2021). However, the catalyst properties will influence the conversion percentage of feed conversion. Shows the influence of reaction temperature on DRM feed conversion.

In another work, Dehimi et al. investigated the effect of temperature on methane dry reforming over 20Mo₁₀Ni/Al₂O₃ catalyst (Dehimi et al., 2020). They found that the methane conversion increased with an increase in temperature. The methane conversion increased from 20 % to 35 % as the temperature increase from 700 °C to 750 °C. The similar trend was reported on the CO₂ conversion but at higher percentages compared to CH₄ conversion. According to those researchers, occurrence of RWGS might be the reason for the situation. However, they also highlighted that the high temperature increase the carbon formation based on the higher H₂/CO ratio. Thus, based on the work of Dehimi et al. , it could be concluded that the high temperature has an advantage on CH₄ and CO₂ conversion but reduce the catalyst stability due to surface carbon formation (Dehimi et al., 2020).

Due to endothermic nature of DRM and RWGS, the high temperature reaction will increase both reaction rate of DRM and RWGS. The H₂/CO ratio can be an indicator on explaining the reaction occurrence. Ali et al. examined the effect of reaction temperature on the H₂/CO ratio of DRM reaction using Ni-SCS catalyst (Ali et al., 2020). The researchers discovered that when the temperature is raised, the ratio of H₂/CO went up as well. Based on the H₂/CO, they concluded that the DRM reaction is more favourable at higher temperature compared to RWGS. However, the existence of RWGS could be observed when H₂/CO ratio was less than unity. The same observation was reported by Damyanova et al. in which the H₂/CO ratio value increased up to 1.79 as the reaction temperature increased form 450 °C to 650 °C (Damyanova et al., 2020).

In summary, it could be concluded that the reaction temperature has an impact on the CH₄ and CO₂ conversions due to the nature of reaction thermodynamic. In addition, H₂/CO molar ratio is also changed and influenced by the competition between the DRM reaction and RWGS reaction. In many cases the carbon formation rate also increases at higher temperature, thus effecting the catalyst stability.

Figure 3: (a)CH₄ conversion, (b)CO₂ conversion, and (c) H₂/CO ratio of Ni/CeO2 with different H₂ reduction temperatures (Zhou et al., 2022)
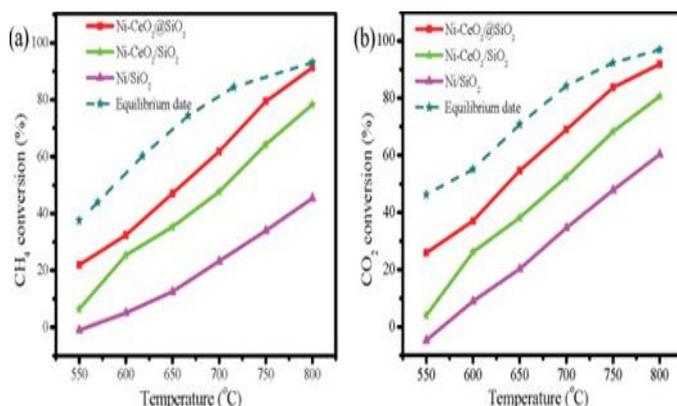
Figure 4: Effect of reaction temperature on DRM feed conversion (Lin et al., 2021).

4.3 Influence of GHSV

According to Fogler, the space time can be defined by following equation (Fogler, 2017):

$$SV = \frac{1}{\tau} \tag{10}$$

where τ is the space time, The space time is equal to the amount of time it takes for each of the reactors to take one reactor volume of fluid and put it into the reactor and space time can be calculated by the following equation:

$$\tau = \frac{V}{v_0} \tag{11}$$

where V is the reactor volume and v_0 is the entering volumetric flow rate. The space time is related to the average time of molecules spent in the reactor.

The average time spent by molecules in the reactor will change the contact time between the reactant and the catalyst's surface, hence affecting the catalyst's performance. Wei et al. examined the effect of GHSV on La-Sr-Cr-NiO for the DRM process and discovered that the conversion of CH₄ and CO₂ increased dramatically from slightly above 80% to almost 90% at 750

°C as GHSV decreased from 1.2 to 0.3 104ml g^{-1}h^{-1} (Wysocka et al., 2019). Increased contact time between the reactants and the surface of the catalyst is primarily responsible for these phenomena. In addition, they discovered that the change in GHSV in this range had no discernible effect on the selectivity of CO and H$_2$, which remained constant at 96%.

Some researchers have also examined the influence of GHSV on the DRM reaction feed conversion and H2/CO ratio (Limlamthong et al., 2020). The impact of GHSV was studied between 24,000 and 72,000 ml/g/h. Due to the decreased residence time for the reactant gases, the rise in GHSV resulted in a decrease in the performance of all catalysts. As the GHSV increased, the conversion of reactant (CH$_4$ and CO$_2$) at lower temperatures decreased substantially. They also evaluated the influence of GHSV at different reaction temperatures and observed that the combination of a high endothermicity of reaction and a short residence time resulted in a very poor conversion of reactants and product yield at low temperatures. In addition, they discovered that the effect of GHSV was more significant at lower temperatures, but the influence of temperature was more significant at higher temperatures, as a substantial increase in catalytic efficiency was found.

The sufficient GHSV is required for reactant activation and performing the reaction. Figure 5 shows the effect of GHSV on CH$_4$ and CO$_2$ conversion over the 10Ni-SiO$_2$@SiO$_2$ catalyst at 700 °C as reported by (Kaviani et al., 2022). The feed conversion and H$_2$/CO ratio decreased as the GHSV increased. The researcher concluded that the main reason for the lower conversion at high GHSV is due to the reduction in contact time between reactant and active phase.

5. CATALYST FORMULATION AND OPERATING CONDITION OPTIMIZATION FOR DRM BY RSM APPROACH

As discussed in previous section, there are many variables that need to be controlled and combined in order to prepare high activity and stability catalyst. Each catalyst formulation and operating condition variable has unique influence on DRM reaction. Currently, there are a lot of experiments that need to be carried out and consume high amount of cost in order to find the relation/interaction effect of each variable on the DRM reaction. Given this, various researchers have used response surface methods to determine the optimal conditions for catalytic methane dry reforming to provide the most hydrogen and syngas.
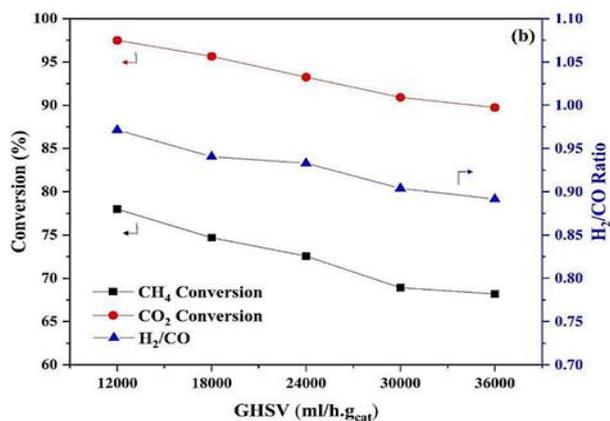
Figure 5: Effect of GSHV on DRM feed conversion and product quality (Kaviani et al., 2022)

Traditionally, variables were optimised by modifying the parameters of one variable while keeping the levels of the other variables constant. This was done in order to get the best possible results. According to Ayodele and Abdullah, the challenges that are linked with the style of chemical process optimization that considers one variable at a time may be avoided by using the response surface approach (RSM) (Figueira et al., 2018). RSM is an optimization method that is more reliable and which provides the statistical design of experiments (DoE) that may be used to achieve the optimum performance of a process. RSM is a strategy for optimising chemical processes that consists of mathematical and statistical techniques. In addition, empirical model fits contribute to the development of an appropriate functional connection between a group of input variables and the desired result.

According to Ayode and Abdullah, the application of RSM for variables optimization involves many steps (Figueira et al., 2018). Initially, the screening procedure is conducted to identify the most relevant characteristics using statistical or literary analysis. This approach prevents picking wrong levels, which might impair process optimization.

The second step involves choosing an experiment design, which may be a three-level factorial design, Box-Behnken design (BBD), central composite design (CCD), or Dohlert design.

Coding the levels of the variables is the next step after selecting an appropriate experimental design. This entails transforming the process's actual values into a coordinate on a dimensionless value scale proportionate to where the experiment is in space. Mathematical and statistical analysis can be done on the data from each experimental point, based on the experimental design chosen. Experiment data are put through mathematical and statistical tests, like ANOVA, to figure out how accurate the model is. Statistical parameters like F-value, P-value, lack of significance, and R^2 can be used to measure how useful a model is that shows a correlation between a variable and a response. The last step in using the RSM is to figure out the best conditions that will give the best response values. In numerical optimization, RSM methods may be used to acquire the intended value for each of the input variables as a function of the desired output. This can be accomplished via the use of numerical optimization. RSM optimization can now be done with computer programmes like Design Expert from Stat Ease and Develve.

Yusuf et al. use RSM approach to investigate the effect of DRM process reaction temperature (600 °C–800 °C) and feed gas ratio (0.5–1.5) on the CH$_4$, CO$_2$ conversions and H$_2$/CO ratio (Yusuf et al., 2022). They used CCD design for experimental design and reported that the experiment data fitted well with reduced quadratic model. The evaluation was based on ANOVA analysis. Each model showed higher F-value and was less than 0.001 P-value. The model is important if its F-value is high, and there is only a 0.01% chance that an F-value this high could be caused by noise. In addition, the ANOVA study revealed that the Lack of Fit F-value was 3.79, which indicates that the Lack of Fit is not significantly compared to the pure error. In addition, the results obtained shows that the coefficient of determination (R^2) and the adjusted R^2 value are 0.9901 and 0.9830, respectively, whereas a standard error of around 2.2% shows good correlation between experimental data and model data.

RSM is an effective tool to evaluate the effect of variables on the response by using mathematic and statistic evaluation. The model graph can be used to visualize the one factor effect and interaction effect of variables on response. In a study on methane dry reforming using oil palm shell activated carbon supported cobalt catalyst Izhab et al., used CCD/RSM to evaluate the effect of operating variables on product yield and quality (Izhab et al., 2021). They used 3D surface graph to visualize the interaction effect between the variables and response as shown in Figure 6. They came to the conclusion that temperature and pressure had a significant influence on the formation of hydrogen gas and carbon monoxide.

By using the model derived from experimental data, RSM is a useful tool to predict the optimum condition in maximizing the response. However, the optimum condition from RSM needs to validate with the experiment and can be accepted if within ±95 % confidence level is achieved. A group researcher used RSM to find the optimum condition for DRM reaction over Ta-promoted Ni/ZSM-5 fibre-like catalyst (Hambali et al., 2021). By employing mathematical and statistical evaluation they have found that the optimum CH$_4$ conversion that was predicted from the response surface analysis was of 96.6 % CH$_4$ conversion at reaction temperature of 784.15 °C, CO$_2$:CH$_4$ feed ratio of 2.52, and GHSV of 33,760 mLg^{-1}h^{-1}. They also reported that, the calculated error between experimental and model simulated result was 0.8 %. Table 2 lists out the previous research that used RSM approach for DRM reaction over catalyst optimization.
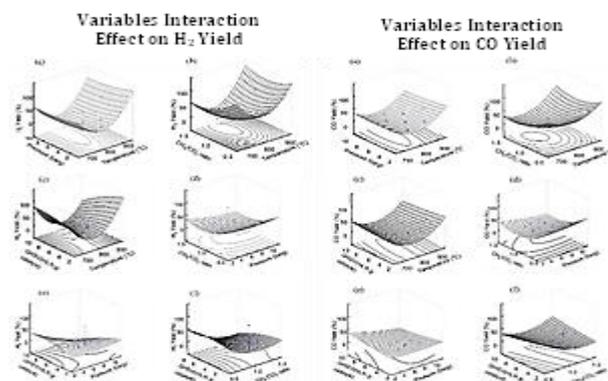
Figure 6: The response surface plot of H$_2$ and CO yield when optimizing each pair of independent variable (a) temperature and gauge pressure (b) temperature and CH$_4$/CO$_2$ ratio (c) temperature and GHSV (d) gauge pressure and CH$_4$/CO$_2$ ratio (e) gauge pressure and GHSV (f) CH$_4$/CO$_2$ ratio and GHSV(Izhab et al., 2021)

6. CATALYST REACTION MECHANISM

A catalyst is a substance that increases or decreases the rate of a chemical reaction without itself being consumed by the reaction. Typically, a catalyst modifies the rate of a reaction by favouring a particular molecular pathway (mechanism) for the reaction. For example, DRM reaction occur at high temperature (850 °C), however, the reaction can occur at lower temperature (600 – 700 °C) with the presence of catalyst. As a consequence of this, the study of catalysts and their applications are critical elements of the ongoing quest for innovative strategies to maximise product yield and selectivity in chemical reactions. With the aid of a catalyst, it is possible to achieve a final product through an alternative pathway with a lower energy barrier. However, catalysts alter only the reaction rate and have no effect on equilibrium. Consequently, in order to comprehend the reaction mechanism of a reaction utilising a certain catalyst, it is necessary to collect data on the reaction rate.

6.1 Steps in Catalytic Reaction

Based on Fogler, the reaction rate or rate law can be developed by understanding steps in catalytic reaction (Fogler, 2017). It is possible to separate the whole of the heterogeneous catalytic reaction process into its constituent elements of; external diffusion, internal diffusion, adsorption of product, surface reaction, desorption of product, internal diffusion of product and external diffusion of product (Najfach et al., 2021; Das, 2018).

It is essential to be aware of the fact that the rate of the mechanism's slowest step is directly related to the rate of the overall response. If the overall rate of reaction is affected by diffusion from the bulk gas or liquid to the catalyst surface or to the mouth of catalyst pores, then changing the flowrate past the catalyst should alter the rate of reaction. It is recommended that the reaction mechanism on the surface of the catalyst be carried out at a higher flow rate in order to eliminate of the effects of diffusion on the reaction rate.

6.2 Mechanism of DRM Reaction over Catalyst

The rate law is the initial step in determining the reaction mechanism of a DRM reaction over a catalyst. The rate law of the DRM reaction may be deduced from experimental data by measuring the reaction rate at various species partial pressures. Some researchers used a differential reactor to evaluate the kinetics of DRM over a Pt-based catalyst (Chen, 2021). The effect of feed partial pressure (CO_2 and CH_4) on the rates of consumption of CH_4 and CO_2 and generation of H_2 and CO was studied between 848 and 898 K by altering the feed partial pressure in the 7.8-39.1 kPa range. According to the experimental results at constant CH_4 partial pressure, increasing CO_2 pressure resulted in greater CH_4 consumption rates, and the relationship between CO_2 consumption rate and partial pressure was linear. The results also revealed that the rates of consumption of CH_4 and CO_2 increased with increasing values of CH_4 partial pressure at constant CO_2 partial pressure, with CH_4 being consumed quicker than CO_2. The rate law can be calculated after conducting a reaction rate experiment utilising a deducing approach or an existing model discriminating.

						Optimum Condition		
RSM DOE	Catalyst	Factors	Low-Level	High-Level	Response	Factors	Response	References
CCD	Oil palm shell activated carbon supported cobalt	Temperature	750 °C	850 °C	H₂ Yield CO Yield	903 °C	82.9 % H₂ 39.6 % CO	Izhab et al., 2021
		Gauge pressure	3 barg	7 barg		0.88 barg		
		CH₄/CO₂ ratio	1.0	1.2		1.31		
		GHSV	3500	5000		4488		
Taguchi	Ni-Ce/TiO2-ZrO2	CH₄/CO₂ ratio	1	2	H₂/CO	2	0.71	Shah and Mondal, 2021
		Temperature	600	800		800		
BBD	Ni-Cu/Al₂O₃	Temperature	700	800	CH₄ Conversion	800	99 %	Rezaei et al., 2019
RCCD	(Ni/DFSBA-15)	Temperature	700	900	H₂/CO	794	0.983	Chong et al., 2020
		GHSV	15000	35000		23815		
		CH4/CO2 Ratio	1	3		1.199		

Table 2: Summary of Literature on Optimization of Syngas Production from Catalytic Reforming of CH_4 And CO_2 Using RSM

Studying the qualitative conclusions that can be drawn from data about the rate at which reactants disappear. or rate of formation of product on the partial pressure of reactants (CH_4 and CO_2) and products (H_2 and CO) may be used to derive the rate law via the deducing method. This method is rarely used by researchers compared to existing model discrimination. Model discrimination method is performed by fitting the experimental data with existing method. Best fit model can be determine using regression technique. There are several theoretical reaction mechanisms that can be selected for DRM reaction such as the power-law model (PL), Eley Rideal (ER) model and Langmuir Hinshelwood-Hougen-Watson (LHHW) model.

The simplest model for calculating the rates of chemical reactions is the one based on kinetic laws (PL), which can only provide an approximate estimate for the relevant parameters. According to the ER model, one of the two reaction gases (methane (CH4) or carbon monoxide (CO2)) is assumed to be absorbed on the catalyst active site first at thermodynamic equilibrium. At that point, the gas at the active site interacts with other gases in the gas phase. A reaction between the adsorbed gas and another reactant is the rate-determining step (RDS). The LHHW model accounts for the absorption of both reaction gases and their subsequent reaction on the catalyst active site. The rate-determining step (RDS) is reached by certain elementary processes, whereas others reach thermodynamic equilibrium (Kweon et al., 2022).

A studied the kinetics and mechanistic of methane dry reforming using a Ca-promoted 1Co-1Ce/AC-N catalyst (Kweon et al., 2022). Three common kinetic models were used to fit the obtained experiment data (Power Law, Eley-Rideal and Langmuir-Hinshelwood). The fitting results demonstrated that the Langmuir-Hinshelwood model provides the best prediction of reforming rates for reaction temperatures ranging from 650 to 800 °C. Table 4 list out the reaction rate equation for each model as published.

6.3 Activation Energy

In order to establish new bonds and activate a chemical reaction, the reactant gas molecules need energy to deform or stretch existing bonds in order to generate new ones. For molecules in reactant gases to form new bonds, they must overcome an energy barrier known as activation energy. The Arrhenius equation may be used to compute activation energy. (Equation 12). The activation energy (Ea) may be calculated using a plot of ln kA as a function of (1/T). In general, the reaction rate is more sensitive to temperature changes when there is a larger activation energy needed. Furthermore, the following formulas will give the specific reaction rate at various temperatures. If $k(T_0)$ and E are known. (13 can be used to calculate the particular reaction rate k(T) at any other temperature (Song, 2010).

$$lnk_a = lnA - \frac{E}{R}\left(\frac{1}{T}\right) \tag{12}$$

$$k(T) = k(T_0)e^{\frac{E}{R}\left(\frac{1}{T_0} - \frac{1}{T}\right)} \tag{13}$$

Numerous studies have been conducted to explore the activation energy over Ni-based catalysts for the CO_2 reforming of CH_4 reaction. Activation energy is an important factor in the process. (Sun et al., 2021; Hambali et al., 2020; Li et al., 2021; Das, 2021; Karam, 2020). As shown by the variation in CH_4 consumption activation energy across supports, supports on Ni crystallites may impact activation energy. The activation energy may vary based on how the catalyst is synthesized (Liang, 2023). CH_4 consumption usually has a larger activation energy than CO_2 consumption, although a promoter can lower it (Kweon et al., 2022). The water-gas shift reaction may affect the apparent activation energy of CO_2 reforming of CH_4.

Table 4: Reaction rate equation based on existing proposed model (Fogler, 2017; Sun et al., 2021)

Model	Reaction Rate Equation	Reference
Power Law	$-r_a = k[P_{CH_4}^{\alpha}][P_{CO_2}^{\beta}]$	Sun et al., 2021
Eley Rideal I	$-r_a = \dfrac{kK_{CO_2}P_{CH_4}P_{CO_2}}{1 + K_{CO_2}P_{CO_2}}$	
Eley Rideal II	$-r_a = \dfrac{kK_{CH_4}P_{CH_4}P_{CO_2}}{1 + K_{CH_4}P_{CH_4}}$	
Langmuir Hishelwood	$-r_a = \dfrac{kK_{CO_2}K_{CH_4}P_{CH_4}P_{CO_2}}{1 + K_{CO_2}P_{CO_2} + K_{CH_4}P_{CH_4}}$	
Dual Site Mechanism	$-r'_{CH_4} = \dfrac{kP_{CH_4}P_{CO_2}}{(1 + K_{CO_2}P_{CO2} + K_{H_2}P_{H_2} + K_{CH_4}P_{CH_4})^2}$	Fogler, 2006
Eley-Rideal	$-r'_{CH_4} = \dfrac{kP_{CH_4}P_{CO_2}}{1 + K_{CO_2}P_{CO_2} + K_{H_2}P_{H_2}}$	

7. SUMMARY

Based on the discussion through this review, the main issues of the present DRM catalyst development are catalytic activity and stability. In many cases, the effort of increased catalyst activity usually resulted in low stability catalyst and vice versa. Continuous effort must be made to improve the DRM catalyst activity and stability by coming up with new catalyst formulation or modification of present catalyst. As discussed in this chapter, there are several routes that can be applied to enhance the performance of DRM catalyst. However, both aspects of economic feasibility and efficiency should be considered.

Since bimetallic nickel-based catalysts, such as Co-Ni catalysts, have demonstrated persistent activity and great resistance to deactivation even in the presence of carbon deposition, they are expected to be the focus of future research in this area. It may also be worthwhile to investigate the possibility of using a Co-Ni bimetallic catalyst supported on a micropores zeolite like Na-A zeolite. To the best of the researchers' knowledge, no such mixtures have ever been documented in the literature. Zeolite with micropores can improve DRM catalyst performance by decreasing particle size and increasing active metal dispersion.

In addition, future efforts should explore the possibility of preventing carbon accumulation within the active metal crystallites while still retaining sufficient activity. This is possible through comprehending the mechanism of catalyst deactivation. The factors that affect the carbon formation were discussed thoroughly in this review. One last thing to consider is that the method used to create the catalyst has a significant impact on how well it performs. When properly prepared, Ni can be dispersed more uniformly on the support, strong metal-support contact can be obtained, catalytic activity can be increased, the material will be stable, and carbon production will be suppressed. More research on optimum and correct preparation techniques of the catalyst is required to prevent coke formation and improve catalyst performance for the DRM process.

REFERENCES

Abdullah, B., Abd Ghani, N.A., and Vo, D. V. N., 2017. Recent advances in dry reforming of methane over Ni-based catalysts. J. Clean. Prod., 162, Pp. 170–185. Doi: 10.1016/j.jclepro.2017.05.176.

Abdullah, N., 2020. Influence of impregnation assisted methods of Ni/SBA-15 for production of hydrogen via dry reforming of methane. Int. J. Hydrogen Energy, 45 (36), Pp. 18426–18439. Doi: 10.1016/j.ijhydene.2019.09.089.

Abdulrasheed, A., 2019. A review on catalyst development for dry reforming of methane to syngas: Recent advances. Renew. Sustain. Energy Rev., 108, Pp. 175–193. Doi: 10.1016/j.rser.2019.03.054.

Abdulrasheed, A.A., Jalil, A.A., Hamid, M.Y.S., Siang, T.J., and Abdullah, T.A.T., 2019. Dry reforming of CH4 over stabilized Ni-La@KCC-1 catalyst: Effects of la promoter and optimization studies using RSM. J. CO2 Util., 37, Pp. 230–239. Doi: 10.1016/j.jcou.2019.12.018.

Afzal, S., Sengupta, D., Sarkar, A., El-Halwagi, M., and Elbashir, N., 2018. Optimization Approach to the Reduction of CO2 Emissions for Syngas Production Involving Dry Reforming. ACS Sustain. Chem. Eng., 6 (6), Pp. 7532–7544. doi: 10.1021/acssuschemeng.8b00235.

Akansu, H., Arbag, H., Tasdemir, H.M., Yasyerli, Y., Yasyerli, N., and Dogu, G., 2021. Nickel-based alumina supported catalysts for dry reforming of biogas in the absence and the presence of H2S: Effect of manganese incorporation. Catal. Today, Pp. 397–399. Doi: 10.1016/j.cattod.2021.12.012.

Al-Fatesh, A.S., 2019. Effect of pre-treatment and calcination temperature on Al2O3-ZrO2 supported Ni-Co catalysts for dry reforming of methane. Int. J. Hydrogen Energy, 44 (39), Pp. 21546–21558. Doi: 10.1016/j.ijhydene.2019.06.085.

Al-Fatesh, A.S., 2022. Effect of Cerium Promoters on an MCM-41-Supported Nickel Catalyst in Dry Reforming of Methane. Ind. Eng. Chem. Res., 61 (1), Pp. 164–174. Doi: 10.1021/acs.iecr.1c03163.

Ali, S., Khader, M.M., Almarri, M.J., and Abdelmoneim, A.G., 2020. Ni-based nano-catalysts for the dry reforming of methane. Catal. Today, 343, Pp. 26–37. Doi: 10.1016/j.cattod.2019.04.066.

Álvarez, M.A., Bobadilla, L.F., Garcilaso, V., Centeno, M.A., and Odriozola, J.A., 2018. CO2 reforming of methane over Ni-Ru supported catalysts: On the nature of active sites by operando DRIFTS study. J. CO2 Util., 24, Pp. 509–515. Doi: 10.1016/j.jcou.2018.01.027.

Alvarez-Galvan, A., 2018. Microwave-assisted coprecipitation synthesis of LaCoO3 nanoparticles and their catalytic activity for syngas production by partial oxidation of methane. Front. Energy Res., 6, Pp. 1–11, 2018, doi: 10.3389/fenrg.2018.00018.

Andraos, S., 2019. Production of hydrogen by methane dry reforming over ruthenium-nickel based catalysts deposited on Al2O3, MgAl2O4, and YSZ. Int. J. Hydrogen Energy, 44 (47), Pp. 25706–25716. doi: 10.1016/j.ijhydene.2019.08.081.

Anil, C., Modak, J.M., and Madras, G., 2020. Syngas production via CO 2 reforming of methane over noble metal (Ru, Pt, and Pd) doped LaAlO 3 perovskite catalyst. Mol. Catal., 484, Pp. 110805. Doi: 10.1016/j.mcat.2020.110805.

Araiza, D. G., Arcos, D. G., Gómez-Cortés, A., and Díaz, G., 2021. Dry reforming of methane over Pt-Ni/CeO2 catalysts: Effect of the metal composition on the stability. Catal. Today, 360, Pp. 46–54. Doi: 10.1016/j.cattod.2019.06.018.

Aramouni, N.A.K., Touma, J.G., Tarboush, B.A., Zeaiter, J., and Ahmad, M.N., 2018. Catalyst design for dry reforming of methane: Analysis review. Renew. Sustain. Energy Rev., 82, Pp. 2570–2585. doi: 10.1016/j.rser.2017.09.076.

Aramouni, N.A.K., Zeaiter, J., Kwapinski, W., Leahy, J. J., and Ahmad, M.N., 2021. Trimetallic Ni-Co-Ru catalyst for the dry reforming of methane: Effect of the Ni/Co ratio and the calcination temperature. Fuel, 300, Pp. 120950. doi: 10.1016/j.fuel.2021.120950.

Ayodele, B.V., and Abdullah, S., 2018. An Overview of Response Surface Methodology Approach to Optimization of Hydrogen and Syngas Production by Catalytic Reforming of Greenhouse Gases (CH4 and CO2). Stat. Approaches with Emphas. Des. Exp. Appl. to Chem. Process., Doi: 10.5772/intechopen.73001.

Aziz, M.A.A., Setiabudi, H.D., Teh, L.P., Annuar, N.H.R., and Jalil, A.A., 2019. A review of heterogeneous catalysts for syngas production via dry reforming. J. Taiwan Inst. Chem. Eng., 101, Pp. 139–158. doi: 10.1016/j.jtice.2019.04.047.

Bagabas, A., 2021. Optimizing MgO Content for Boosting γ-Al2O3-Supported Ni Catalyst in Dry Reforming of Methane. Catalysts, 11 (10). Doi: 10.3390/catal11101233.

Bian, Z., Das, S., Wai, M.H., Hongmanorom, P., and Kawi, S., 2017. A Review on Bimetallic Nickel-Based Catalysts for CO2 Reforming of Methane. Chem. Phys. Chem., 8 (22), Pp. 3117–3134. Doi: 10.1002/cphc.201700529.

Cabascango, V.E.Q., and Bazhin, V.Y., 2020. Nickel oxide reduction in CO/CO2 gas mixtures in reverberatory furnaces. J. Phys. Conf. Ser., 1515 (2), Pp. 22028. doe: 10.1088/1742-6596/1515/2/022028.

Chamoumi, M., Abatzoglou, N., Blanchard, J., Iliuta, M.C., and Larachi, F., 2017. Dry reforming of methane with a new catalyst derived from a negative value mining residue spinellized with nickel. Catal. Today, 291, Pp. 86–98. doi: 10.1016/j.cattod.2017.02.018.

Charisiou, N.D., Iordanidis, A., Polychronopoulou, K., Yentekakis, I.V., and Goula, M.A., 2018. Studying the stability of Ni supported on modified with CeO2 alumina catalysts for the biogas dry reforming reaction. Mater. Today, Proc., 5 (4), Pp. 27607–27616. Doi: 10.1016/j.matpr.2018.09.081.

Chen, H., 2021. Structured silicalite-1 encapsulated Ni catalyst supported on SiC foam for dry reforming of methane. AIChE J., 67 (4), Pp. e17126. Doi: https://doi.org/10.1002/aic.17126.

Chong, C.C., Cheng, Y.W., Setiabudi, H.D., Ainirazali, N., Vo, D.V.N., and Abdullah, B., 2020. Dry reforming of methane over Ni/dendritic fibrous SBA-15 (Ni/DFSBA-15): Optimization, mechanism, and regeneration studies. Int. J. Hydrogen Energy, 45 (15), Pp. 8507–8525. Doi: 10.1016/j.ijhydene.2020.01.056.

Chu, S., 2020. Sinter-resistant Rh nanoparticles supported on γ-Al2O3nanosheets as an efficient catalyst for dry reforming of methane. Nanoscale, 12 (40), Pp. 20922–20932. Doi: 10.1039/d0nr04644b.

Damyanova, S., Shtereva, I., Pawelec, B., Mihaylov, L., and Fierro, J.L.G., 2020. Characterization of none and yttrium-modified Ni-based catalysts for dry reforming of methane. Appl. Catal. B. Environ., 278, Pp. 119335. Doi: 10.1016/j.apcatb.2020.119335.

Das, S., 2018. Silica–Ceria sandwiched Ni core–shell catalyst for low temperature dry reforming of biogas: Coke resistance and mechanistic insights. Appl. Catal. B Environ., 230, Pp. 220–236. Doi: 10.1016/j.apcatb.2018.02.041.

Das, S., 2021. Role of lattice oxygen in methane activation on Ni-phyllosilicate@Ce1-xZrxO2 core-shell catalyst for methane dry reforming: Zr doping effect, mechanism, and kinetic study. Appl. Catal. B Environ., 290, Pp. 119998. doi: https://doi.org/10.1016/j.apcatb.2021.119998.

de Araújo Moreira, T.G., de Carvalho Filho, J.F.S., Carvalho, Y., de Almeida, J.M.A.R., Romano, P.N., and Sousa-Aguiar, E.F., 2021. Highly stable low noble metal content rhodium-based catalyst for the dry reforming of methane. Fuel, 287. Doi: 10.1016/j.fuel.2020.119536.

de Souza, M.G., 2022. NiO–MgAl2O4 systems for dry reforming of methane: Effect of the combustion synthesis route in the catalysts properties. Mater. Chem. Phys., 278, Pp. 125599. Doi: https://doi.org/10.1016/j.matchemphys.2021.125599.

de Vasconcelos, B.R., Minh, D.P., Martins, E., Germeau, A., Sharrock, P., and Nzihou, A., 2020. Highly efficient hydroxyapatite-supported nickel catalysts for dry reforming of methane. Int. J. Hydrogen Energy, 45 (36), Pp. 18502–18518. doi: 10.1016/j.ijhydene.2019.08.068.

Dębek, R., Motak, M., Galvez, M.E., Grzybek, T., and Da Costa, P., 2017. Influence of Ce/Zr molar ratio on catalytic performance of hydrotalcite-derived catalysts at low temperature CO2 methane reforming. Int. J. Hydrogen Energy, 42 (37), Pp. 23556–23567. Doi: 10.1016/j.ijhydene.2016.12.121.

Dehimi, L., Gaillard, M., Virginie, M., Erto, A., and Benguerba, Y., 2020. Investigation of dry reforming of methane over Mo-based catalysts. Int. J. Hydrogen Energy, 45 (46), Pp. 24657–24669. doi: 10.1016/j.ijhydene.2020.06.203.

Erdogan, B., Arbag, H., and Yasyerli, N., 2017. SBA-15 supported mesoporous Ni and Co catalysts with high coke resistance for dry reforming of methane. Int. J. Hydrogen Energy, 43 (3), Pp. 1396–1405. doi: 10.1016/j.ijhydene.2017.11.127.

Figueira, C.E., Moreira, P.F., Giudici, R., Alves, R.M.B., and Schmal, M., 2018. Nanoparticles of Ce, Sr, Co in and out the multi-walled carbon nanotubes applied for dry reforming of methane. Appl. Catal. A Gen., 550, Pp. 297–307. doi: 10.1016/j.apcata.2017.11.019.

Fogler, H.S., 2017. Essentials of Chemical Reaction Engineering. Pearson Education.

Gaillard, M., Virginie, M., and Khodakov, A.Y., 2017. New molybdenum-based catalysts for dry reforming of methane in presence of sulfur: A promising way for biogas valorization. Catal. Today, 289, Pp. 143–150. doi: 10.1016/j.cattod.2016.10.005.

Gao, Y., 2020. A novel nickel catalyst supported on activated coal fly ash for syngas production via biogas dry reforming. Renew. Energy, 149, Pp. 786–793. Doi: 10.1016/j.renene.2019.12.096.

Ghani, A.A., Torabi, F., and Ibrahim, H., 2018. Autothermal reforming process for efficient hydrogen production from crude glycerol using nickel supported catalyst: Parametric and statistical analyses. Energy, 144, Pp. 129–145. Doi: 10.1016/j.energy.2017.11.132.

Guerrero-Caballero, J., Kane, T., Haidar, N., Jalowiecki-Duhamel, L., and Löfberg, A., 2019. Ni, Co, Fe supported on Ceria and Zr doped Ceria as oxygen carriers for chemical looping dry reforming of methane. Catal. Today, 333, Pp. 251–258. doi: 10.1016/j.cattod.2018.11.064.

Guharoy, U., Le Saché, E., Cai, Q., Reina, T. R., and Gu, S., 2018. Understanding the role of Ni-Sn interaction to design highly effective CO2 conversion catalysts for dry reforming of methane. J. CO2 Util., 27, Pp. 1–10. Doi: 10.1016/j.jcou.2018.06.024.

Hambali, H.U., Jalil, A.A., Abdulrasheed, A.A., Siang, T.J., and Vo, D.V.N., 2020. Enhanced dry reforming of methane over mesostructured fibrous Ni/MFI zeolite: Influence of preparation methods. J. Energy Inst., 93 (4), Pp. 1535–1543. Doi: https://doi.org/10.1016/j.joei.2020.01.016.

Hambali, H.U., Jalil, A.A., Abdulrasheed, A.A., Siang, T.J., Gambo, Y., and Umar, A.A., 2022. Zeolite and clay based catalysts for CO2 reforming of methane to syngas: A review. Int. J. Hydrogen Energy, 47 (72), Pp. 30759–30787. doi: 10.1016/j.ijhydene.2021.12.214.

Hambali, H.U., Jalil, A.A., Abdulrasheed, A.A., Siang, T.J., Owgi, A.H.K., and Aziz, F.F.A., CO2 reforming of methane over Ta-promoted Ni/ZSM-5 fibre-like catalyst: Insights on deactivation behaviour and optimization using response surface methodology (RSM). Chem. Eng. Sci., 231, Pp. 116320. doi: 10.1016/j.ces.2020.116320.

Han, B., Zhong, J., Li, W., Zhang, Z., Bi, G., and Xie, J., 2021. The promotional role of β-cyclodextrin on Ni-Mo2C/MgO catalyst for biogas reforming. Mol. Catal., 515. Doi: 10.1016/j.mcat.2021.111897.

Han, J.W., Park, J.S., Choi, M.S., and Lee, H., 2017. Uncoupling the size and support effects of Ni catalysts for dry reforming of methane. Appl. Catal. B Environ., 203, Pp. 625–632. doi: 10.1016/j.apcatb.2016.10.069.

Izhab, I., Asmadi, M., and Amin, N.A.S., 2021. Methane dry reforming using oil palm shell activated carbon supported cobalt catalyst: multi-response optimization. Int. J. Hydrogen Energy, 46 (48), Pp. 24754–24767. doi: 10.1016/j.ijhydene.2020.04.188.

Jabbour, K., Saad, A., Inaty, L., Davidson, A., Massiani, P., and El Hassan, N., 2019. Ordered mesoporous Fe-Al2O3 based-catalysts synthesized via a direct 'one-pot' method for the dry reforming of a model biogas mixture. Int. J. Hydrogen Energy, 44 (29), Pp. 14889–14907.

Jawad, A., Rezaei, F., and Rownaghi, A. A., 2020. Highly efficient Pt/Mo-Fe/Ni-based Al2O3-CeO2 catalysts for dry reforming of methane. Catal. Today, 350, Pp. 80–90. Doi: 10.1016/j.cattod.2019.06.004.

Jing, J.Y., Yang, Z.F., Huo, J.M., Bai, H.C., and Li, Y.W., 2019. Metal precursor impregnation sequence effect on the structure and performance of Ni–Co/MgO catalyst. Int. J. Hydrogen Energy, 44 (16), Pp. 8089–8098. Doi: 10.1016/j.ijhydene.2019.02.079.

Joo, S., Kwon, O., Kim, S., Jeong, H.Y. and Kim, G., 2020. Ni-Fe Bimetallic Nanocatalysts Produced by Topotactic Exsolution in Fe deposited PrBaMn 1.7 Ni 0.3 O 5+ δ for Dry Reforming of Methane. J. Electrochem. Soc., 167 (6), Pp. 064518. doi: 10.1149/1945-

7111/ab8390.

Jung, S., Lee, J., Moon, D.H., Kim, K.H., and Kwon, E.E., 2020. Upgrading biogas into syngas through dry reforming. Renew. Sustain. Energy Rev., 143, Pp. 110949. Doi: 10.1016/j.rser.2021.110949.

Kalai, D.Y., Stangeland, K., Jin, Y., Tucho, W.M., and Yu, Z., 2018. Biogas dry reforming for syngas production on La promoted hydrotalcite-derived Ni catalysts. Int. J. Hydrogen Energy, 43 (42), Pp. 19438–19450. Doi: 10.1016/j.ijhydene.2018.08.181.

Karam, L., 2020. Comprehensive study on the effect of magnesium loading over nickel-ordered mesoporous alumina for dry reforming of methane. Energy Convers. Manag., 225, Pp. 113470. doi: 10.1016/j.enconman.2020.113470.

Karemore, A.L., Sinha, R., Chugh, P., and Vaidya, P.D., 2022. Syngas production by carbon dioxide reforming of methane over Pt/Al2O3 and Pt/ZrO2-SiO2 catalysts. Chem. Eng. Sci., 249. Doi: 10.1016/j.ces.2021.117347.

Kaviani, M., Rezaei, M., Alavi, S.M., and Akbari, E., 2022. High coke resistance Ni-SiO2@SiO2 core-shell catalyst for biogas dry reforming: Effects of Ni loading and calcination temperature. Fuel, 330, Pp. 125609. doi: 10.1016/j.fuel.2022.125609.

Khatri, J., 2021. Ceria promoted phosphate-zirconia supported Ni catalyst for hydrogen rich syngas production through dry reforming of methane. Int. J. Energy Res., 45 (13), Pp. 19289–19302. Doi: 10.1002/er.7026.

Kim, S.M., 2017. Cooperativity and dynamics increase the performance of NiFe dry reforming catalysts. J. Am. Chem. Soc., 139 (5), Pp. 1937–1949. Doi: 10.1021/jacs.6b11487.

Kumar, N., Kanitkar, S., Wang, Z., Haynes, D., Shekhawat, D., and Spivey, J.J., 2019. Dry reforming of methane with isotopic gas mixture over Ni-based pyrochlore catalyst. Int. J. Hydrogen Energy, 44 (8), Pp. 4167–4176. Doi: 10.1016/j.ijhydene.2018.12.145.

Kweon, S., Kim, Y.W., Shin, C.H., Park, M.B., and Min, H.K., 2022. Nickel silicate beta zeolite prepared by interzeolite transformation: A highly active and stable catalyst for dry reforming of methane. Chem. Eng. J., 431 (P3), Pp. 133364. Doi: 10.1016/j.cej.2021.133364.

Kweon, S., Kim, Y.W., Shin, C.H., Park, M.B., and Min, N.K., 2022. Nickel silicate beta zeolite prepared by interrelate transformation: A highly active and stable catalyst for dry reforming of methane. Chem. Eng. J., 431, Pp. 133364. doi: https://doi.org/10.1016/j.cej.2021.133364.

Lee, S.M., Won, J.M., Kim, G.M., Lee, S.H., Kim, S.S., and Hong, S.C., 2017. Improving carbon tolerance of Ni-YSZ catalytic porous membrane by palladium addition for low temperature steam methane reforming. Appl. Surf. Sci., 419, Pp. 788–794. doi: 10.1016/j.apsusc.2017.05.039.

Li, B., Yuan, Y., Li, L., Li, B., Wang, X., and Tomishige, K., 2021. Lanthanide oxide modified nickel supported on mesoporous silica catalysts for dry reforming of methane. Int. J. Hydrogen Energy, 46 (62), Pp. 31608–31622. doi: https://doi.org/10.1016/j.ijhydene.2021.07.056.

Liang, D., 2023. Dry reforming of methane for syngas production over attapulgite-derived MFI zeolite encapsulated bimetallic Ni-Co catalysts. Appl. Catal. B Environ., 322, Pp. 122088. Doi: https://doi.org/10.1016/j.apcatb.2022.122088.

Limlamthong, M., Tesana, S., and Yip, A.C.K., 2020. Metal encapsulation in zeolite particles: A rational design of zeolite-supported catalyst with maximum site activity. Adv. Powder Technol., 31 (3), Pp. 1274–1279. doi: https://doi.org/10.1016/j.apt.2020.01.006.

Lin, S., 2021. Trifunctional strategy for the design and synthesis of a Ni-CeO2@SiO2 catalyst with remarkable low-temperature sintering and coking resistance for methane dry reforming. Chinese J. Catal., 42 (10), Pp. 1808–1820. doi: https://doi.org/10.1016/S1872-2067(21)63789-0.

Ma, Q., 2020. Stabilizing Ni on bimodal mesoporous-macroporous alumina

with enhanced coke tolerance in dry reforming of methane to syngas. J. CO2 Util., 35, Pp. 288–297. Doi: 10.1016/j.jcou.2019.10.010.

Mazhar, A., 2021. Performance Analysis of TiO2-Modified Co/MgAl2O4 Catalyst for Dry Reforming of Methane in a Fixed Bed Reactor for Syngas (H2, CO) Production. Energies, 14 (11), Doi: 10.3390/en14113347.

Mofrad, B.D., Rezaei, M., and Hayati-Ashtiani, M., 2019. Preparation and characterization of Ni catalysts supported on pillared nanoporous bentonite powders for dry reforming reaction. Int. J. Hydrogen Energy, 44 (50), Pp. 27429–27444. Doi: 10.1016/j.ijhydene.2019.08.194.

Moogi, S., Ko, C.H., Rhee, C.H., Jeon, B.H., Khan, M.A., and Park, Y.K., 2022. Influence of catalyst synthesis methods on anti-coking strength of perovskites derived catalysts in biogas dry reforming for syngas production. Chem. Eng. J., 437 (1), Pp. 135348. Doi: 10.1016/j.cej.2022.135348.

Moreno, A.A., Ramirez-Reina, T., Ivanova, S., Roger, A.C., Centeno, M.A., and Odriozola, J.A., 2021. Bimetallic Ni–Ru and Ni–Re Catalysts for Dry Reforming of Methane: Understanding the Synergies of the Selected Promoters. Front. Chem., 9, Pp. 1–10. Doi: 10.3389/fchem.2021.694976.

Najfach, A.J., Almquist, C.B., and Edelmann, R.E., 2021. Effect of Manganese and zeolite composition on zeolite-supported Ni-catalysts for dry reforming of methane. Catal. Today, 369, Pp. 31–47. Doi: https://doi.org/10.1016/j.cattod.2020.07.058.

Nisa, K.S., 2022. Effect of base promoter on activity of MCM-41-supported nickel catalyst for hydrogen production via dry reforming of methane. Int. J. Hydrogen Energy, 47 (55), Pp. 23201–23212. doi: 10.1016/j.ijhydene.2022.05.081.

Ocsachoque, M.A., Aparicio, M.S.L., and Gonzalez, M.G., 2017. Effect of Rh Addition to Ni/MgO-Al 2 O 3 Catalysts for Dry Reforming of Methane. Indian J. Sci. Technol., 10 (12), Pp. 1–9. doi: 10.17485/ijst/2017/v10i12/107464.

Pan, C., Guo, Z., Dai, H., Ren, R., and Chu, W., 2020. Anti-sintering mesoporous Ni–Pd bimetallic catalysts for hydrogen production via dry reforming of methane. Int. J. Hydrogen Energy, 45 (32), Pp. 16133–16143. Doi: 10.1016/j.ijhydene.2020.04.066.

Park, J.H., Yeo, S., Kang, T.J., Shin, H.R., Heo, I., and Chang, T.S., 2017. Effect of Zn promoter on catalytic activity and stability of Co/ZrO2 catalyst for dry reforming of CH4. J. CO2 Util., 23, Pp. 10–19. Doi: 10.1016/j.jcou.2017.11.002.

Pham, C.Q., Ngoc, A., Cao, T., Phuong, P.T.T., Tuong, T., and Tran, V., 2022. Enhancement of syngas production from dry reforming of methane over Co / Al 2 O 3 catalyst: Insight the promotional effects of europium and neodymium. J. Energy Inst., 105, Pp. 314–322. Doi: 10.1016/j.joei.2022.10.004.

Phan, T.S., 2018. Hydroxyapatite supported bimetallic cobalt and nickel catalysts for syngas production from dry reforming of methane. Appl. Catal. B Environ., 224, Pp. 310–321. doi: 10.1016/j.apcatb.2017.10.063.

Ponugoti, P.V., and Janardhanan, V.M., 2020. Mechanistic kinetic model for biogas dry reforming. Ind. Eng. Chem. Res., 59 (33), Pp. 14737–14746. Doi: 10.1021/acs.iecr.0c02433.

Rezaei, R., Moradi, G., and Sharifnia, S., 2019. Dry Reforming of Methane over Ni-Cu/Al2O3 Catalyst Coatings in a Microchannel Reactor: Modelling and Optimization Using Design of Experiments. Energy and Fuels, 33 (7), Pp. 6689–6706. Doi: 10.1021/acs.energyfuels.9b00692.

Sápi, A., 2019. Noble-metal-free and Pt nanoparticles-loaded, mesoporous oxides as efficient catalysts for CO 2 hydrogenation and dry reforming with methane. J. CO2 Util., 32, Pp. 106–118. doi: 10.1016/j.jcou.2019.04.004.

Shah, M., and Mondal, P., 2021. Optimization of CO2 reforming of methane

process for the syngas production over Ni–Ce/TiO2–ZrO2 catalyst using the Taguchi method. Int. J. Hydrogen Energy, 46 (44), Pp. 22799–22812. doi: 10.1016/j.ijhydene.2021.04.091.

Sharifianjazi, F., 2021. A review on recent advances in dry reforming of methane over Ni- and Co-based nanocatalysts. Int. J. Hydrogen Energy, doi: https://doi.org/10.1016/j.ijhydene.2021.11.172.

Sharma, H., and Dhir, A., 2020. Hydrogen augmentation of biogas through dry reforming over bimetallic nickel-cobalt catalysts supported on titania. Fuel, 279, Pp. 118389. Doi: 10.1016/j.fuel.2020.118389.

Shin, S.A., 2018. Dry reforming of methane over Ni/ZrO2-Al2O3 catalysts: Effect of preparation methods. J. Taiwan Inst. Chem. Eng., 90, Pp. 25–32. doi: 10.1016/j.jtice.2017.11.032.

Singha, R.K., Yadav, A., Shukla, A., Kumar, M., and Bal, R., 2017. Low temperature dry reforming of methane over Pd-CeO2 nanocatalyst," Catal. Commun., 92, Pp. 19–22. doi: 10.1016/j.catcom.2016.12.019.

Song, H.S., 2010. CH 4 Reforming for Synthesis Gas Production over Supported Ni Catalysts.

Sun, Y., Zhang, G., Cheng, H., Liu, J., and Li, G., 2021. Kinetics and mechanistic studies of methane dry reforming over Ca promoted 1Co–1Ce/AC-N catalyst. Int. J. Hydrogen Energy, 46 (1), Pp. 531–542. Doi: 10.1016/j.ijhydene.2020.09.192.

Sun, Y., Zhang, G., Xu, Y., and Zhang, R., 2019. Dry reforming of methane over Co-Ce-M/AC-N catalyst: Effect of promoters (Ca and Mg) and preparation method on catalytic activity and stability. Int. J. Hydrogen Energy, 44 (41), Pp. 22972–22982. Doi: 10.1016/j.ijhydene.2019.07.010.

Taherian, Z., Khataee, A., and Orooji, Y., 2021. Nickel-based nano catalysts promoted over MgO-Modi fi ed SBA-16 for dry reforming of methane for syngas production: Impact of support and promoters. J. Energy Inst., 97, Pp. 100–108. doi: 10.1016/j.joei.2021.04.005.

Taherian, Z., Yousefpour, M., Tajally, M., and Khoshandam, B., 2017. Catalytic performance of Samaria-promoted Ni and Co/SBA-15 catalysts for dry reforming of methane. Int. J. Hydrogen Energy, 42 (39), Pp. 24811–24822. doi: 10.1016/j.ijhydene.2017.08.080.

Tran, N.T., 2021. CO2 Reforming of CH4 on Mesoporous Alumina-Supported Cobalt Catalyst: Optimization of Lanthana Promoter Loading. Top. Catal., 64 (5), Pp. 338–347. doi: 10.1007/s11244-021-01428-x.

Turap, Y., Wang, I., Fu, T., Wu, Y., Wang, Y., and Wang, W., 2020. Co–Ni alloy supported on CeO2 as a bimetallic catalyst for dry reforming of methane. Int. J. Hydrogen Energy, 45 (11), Pp. 6538–6548. doi: 10.1016/j.ijhydene.2019.12.223.

Wang, F., 2017. Enhanced catalytic performance of Ir catalysts supported on ceria-based solid solutions for methane dry reforming reaction. Catal. Today, 281, Pp. 295–303. Doi: 10.1016/j.cattod.2016.03.055.

Wang, F., 2020. Low Temperature CO2Reforming with Methane Reaction over CeO2-Modified Ni@SiO2Catalysts. ACS Appl. Mater. Interfaces, 12 (31), Pp. 35022–35034. Doi: 10.1021/acsami.0c09371.

Wang, H., Dong, X., Zhao, T., Yu, H., and Li, M., 2019. Dry reforming of methane over bimetallic Ni-Co catalyst prepared from La (CoxNi1-x)0.5Fe0.5O3 perovskite precursor: Catalytic activity and coking resistance. Appl. Catal. B Environ., 245, Pp. 302–313. doi: 10.1016/j.apcatb.2018.12.072.

Wei, T., Jia, L., Luo, J.L., Chi, B., Pu, J., and Li, J., 2020. CO2 dry reforming of CH4 with Sr and Ni co-doped LaCrO3 perovskite catalysts. Appl. Surf. Sci., 506, Pp. 144699. Doi: https://doi.org/10.1016/j.apsusc.2019.144699.

Wysocka, I., Hupka, J., and Rogala, A., 2019. Catalytic Activity of Nickel and Ruthenium–Nickel Catalysts Supported on SiO2, ZrO2, Al2O3, and MgAl2O4 in a Dry Reforming Process. Catalysts, 9 (6). doi: 10.3390/catal9060540.

Xie, C., 2020. Defect Chemistry in Heterogeneous Catalysis: Recognition, Understanding, and Utilization. ACS Catalysis, 10 (19), Pp. 11082–11098. doi: 10.1021/acscatal.0c03034.

Xie, Y., 2021. Enhanced catalytic performance of methane combustion over zeolite supported Pd catalysts with the lanthanum. Catal. Today, 364, Pp. 16–20. Doi: 10.1016/j.cattod.2019.11.030.

Yentekakis, I.V., Panagiotopoulou, P., and Artemakis, G., 2021. A review of recent efforts to promote dry reforming of methane (DRM) to syngas production via bimetallic catalyst formulations," Appl. Catal. B Environ., 296, Pp. 120210. doi: https://doi.org/10.1016/j.apcatb.2021.120210.

Yusuf, M., Farooqi, A.S., Alam, M.A., Keong, L.K., Hellgardt, K., and Abdullah, B., 2021. Performance of Ni/Al2O3-MgO catalyst for Dry Reforming of Methane: Effect of preparation routes. IOP Conf. Ser. Mater. Sci. Eng., 1092 (1), Pp. 12069. Doi: 10.1088/1757-899X/1092/1/012069.

Yusuf, M., Farooqi, A.S., Alam, M.A., Keong, L.K., Hellgardt, K., and Abdullah, B., 2022. Response surface optimization of syngas production from greenhouse gases via DRM over high performance Ni–W catalyst. Int. J. Hydrogen Energy, 47 (72), Pp. 31058–31071. Doi: 10.1016/j.ijhydene.2021.05.153.

Zhai, P., 2021. Development of direct conversion of syngas to unsaturated hydrocarbons based on Fischer-Tropsch route. Chem, 7 (11), Pp. 3027–3051. Doi: 10.1016/j.chempr.2021.08.019.

Zhang, S., 2021. Robust nanosheet-assembled Al2O3-supported Ni catalysts for the dry reforming of methane: the effect of nickel content on the catalytic performance and carbon formation. New J. Chem., 45 (46), Pp. 21750–21762. doi: 10.1039/D1NJ03954G.

Zhou, H., 2018. A single source method to generate Ru-Ni-MgO catalysts for methane dry reforming and the kinetic effect of Ru on carbon deposition and gasification. Appl. Catal. B Environ., 233, Pp. 143–159. Doi: 10.1016/j.apcatb.2018.03.103.

Zhou, R., Mohamedali, M., Ren, Y., Lu, Q., and Mahinpey, N., 2022. Facile synthesis of multi-layered nanostructured Ni/CeO2 catalyst plus in-situ pre-treatment for efficient dry reforming of methane. Appl. Catal. B. Environ., 316, Pp. 121696. doi: https://doi.org/10.1016/j.apcatb.2022.121696.